Environmental Science and Pollution Research (2022) 29:3213–3229
https://doi.org/10.1007/s11356-021-17042-z

REVIEW ARTICLE

Biogenic metal nanoparticles with microbes and their applications in water treatment: a review

Zhiling Du[1,2] · Yunhai Zhang[1] · Anlin Xu[1] · Shunlong Pan[1] · Yongjun Zhang[1]

Received: 8 March 2021 / Accepted: 11 October 2021 / Published online: 3 November 2021

Abstract

Due to their unique characteristics, nanomaterials are widely used in many applications including water treatment. They are usually synthesized via physiochemical methods mostly involving toxic chemicals and extreme conditions. Recently, the biogenic metal nanoparticles (Bio-Me-NPs) with microbes have triggered extensive exploration. Besides their environmental-friendly raw materials and ambient biosynthesis conditions, Bio-Me-NPs also exhibit the unique surface properties and crystalline structures, which could eliminate various contaminants from water. Recent findings in the synthesis, morphology, composition, and structure of Bio-Me-NPs have been reviewed here, with an emphasis on the metal elements of Fe, Mn, Pd, Au, and Ag and their composites which are synthesized by bacteria, fungi, and algae. Furthermore, the mechanisms of eliminating organic and inorganic contaminants with Bio-Me-NPs are elucidated in detail, including adsorption, oxidation, reduction, and catalysis. The scale-up applicability of Bio-Me-NPs is also discussed.

Keywords Emerging contaminants · Metal oxides · Trace pollutants · Heavy metals · Nanoparticles · Pharmaceuticals

Introduction

Nanomaterials possess unique optoelectronic, physiochemical, and biological properties compared with their macroscopic counterparts (Menon et al. 2017). Therefore, they have been widely applied in many applications including eliminating pollutants from water and wastewater (Krishnaraj et al. 2014; Kumar et al. 2014; Suresh et al. 2011). For example, the carbon nanotube obtained 50 times higher pseudo-first-order reaction constant than that of granular activated carbon in the degradation of acetaminophen by activating persulfate (1.5 m^{-1} g^{-1} vs 0.03 m^{-1} g^{-1}) (Pham et al. 2020). Also, in order to constrain the fast recombination of photon-generated carriers, tuning the particle size of TiO_2 into the nanometer range can enhance the transfer of interfacial charge carrier effectively (Qu et al. 2013).

However, the nanomaterials are mostly synthesized with physicochemical processes which may involve hazardous and costly chemicals as reducing, capping, or stabilizing agents, and the extreme conditions like high temperature and high pressure (Menon et al. 2017; Murphy et al. 2005; Rajeshkumar & Bharath 2017). Considering the drawbacks of traditional strategies, many researchers made efforts to employ environment-friendly and cost-effective protocols for nanomaterial production.

Biosynthesis is an important alternative protocol. Many microbes like bacteria, fungi, and algae can mediate the reduction and oxidation of metal ions with the formation of biogenic metal nanoparticles (Bio-Me-NPs) (Tani et al. 2004; Veeramani et al. 2013). Microorganisms and their intracellular or extracellular enzymes can replace exogenous reducing and capping or stabilizing agent and play a key role in changing the valency and morphology of Bio-Me-NPs

Responsible Editor: Gerald Thouand

Highlights
Bio-Me-NPs can exhibit superior properties to chemically synthesized peer materials.
The morphology and biosynthesis of Bio-Me-NPs are systematically reviewed.
The mechanisms of eliminating contaminants with Bio-Me-NPs are discussed in detail.
The scale-up applicability of Bio-Me-NPs is highlighted.

✉ Yongjun Zhang
y.zhang@njtech.edu.cn

[1] School of Environmental Science and Engineering, Nanjing Tech University, Nanjing 211800, People's Republic of China

[2] School of the Environment, Nanjing University, Nanjing 210023, People's Republic of China

(Andeer et al. 2015; Sarkar et al. 2012; Zhang et al. 2015b). In addition, biosynthesis usually can be conducted under ambient conditions, like room temperature, no pressure control, and neutral pH (Furgal et al. 2015; Gericke & Pinches 2006; Matsushita et al. 2018). More interestingly, Bio-Me-NPs may demonstrate some better capacities owing to their unique characteristics like higher specific surface, broader vacancy range, and more crystal defects than their chemically synthesized peers. For instance, the dechlorination of carbon tetrachloride by biogenic FeS derived from *Shewanella putrefaciens* CN32 was 5 times faster than abiotic FeS, which was ascribed to the higher reductive content (structural Fe(II) and disulfide) and well dispersity of biogenic FeS (Huo et al. 2016). The specific area of biogenic magnetite was 20-fold higher than that of the synthetic magnetite while the adsorption capacity of heavy metals was consequently 30 ~ 40-fold higher (Iwahori et al. 2014). The superior capacity of Bio-Me-NPs is also investigated in advanced oxidation process (AOPs) as catalysts. With respect to the phenol degradation by persulfate activation, the reaction rate constant (10.5×10^{-2} min^{-1}) with biogenic manganese oxide as catalyst is higher than serval abiotic Mn-based catalysts ($0.4 \sim 8.7 \times 10^{-2}$ min^{-1}) (Liu et al. 2016; Saputra et al. 2013, 2014; Tian et al. 2018; Wang et al. 2015).

Several reviews have been published so far on the related topics. Ten years ago, Hennebel et al. (2009a) reviewed the biosynthesis of biogenic Fe, Mn, Pd, Pt, Au, and Ag NPs and discussed their applications in AOPs. In the review of Gautam et al. (2019), the applications of biogenic particles in the remediation of water pollution are highlighted but less content are spent on the progress of the biosynthesis and the morphology of Bio-Me-NPs. Recently, Sadhasivam et al. (2020) reviewed the synthesis of Bio-Fe-NPs and other metals were not included. They also briefly summarized the general application of Bio-Fe-NPs and the water treatment was not a focus. We are here trying to review the advances on the biosynthesis of metal NPs mediated by microbes including bacteria, fungi, and algae; the morphology and composition of the NPs; and the applications on the elimination of organic and inorganic contaminants, mainly consisting of emerging organic contaminants and heavy metals. Besides, the scale-up applicability of Bio-Me-NPs is also discussed.

Types and morphology

The widely studied Bio-Me-NPs mainly include the metals like Fe, Mn, Pb, Au, and Ag. Their biogenic source, morphology, size, and chemical valence are summarized in Table 1 and are further discussed in below sections.

Bio-Fe-NPs

Microbes play an important role in the geochemical cycle of iron. With its wide valences, Fe could be an electron acceptor or donor, depending on the oxidation environment, e.g., anoxic or oxic conditions. As a result, Fe can exist with the valency of 0, II, III, and IV in Bio-Fe-NPs (Huo et al. 2016; Tuo et al. 2015; Watts et al. 2015). The size of Bio-Fe-NPs may range from few nanometers to dozens of nanometers. With the aid of transmission electron microscope (TEM), scanning electron microscope (SEM), and atomic force microscopy (AFM), researchers identified various shapes of Bio-Fe-NPs, such as hollow tubular, spherical, and irregular forms (Bai et al. 2016; Jung et al. 2008; Pi et al. 2017). As shown in Fig. S1, hollow tubular Bio-Fe-NPs derived from *Leptothrix* sp. are coating on the sheath of a filamentous bacterium to support its premise (Hargreaves & Alharthi 2016; Rentz et al. 2009). Another research found that the biogenic Mackinawite synthesized by *S. putrefaciens* CN32 aggregated to form rosette-like particles (Veeramani et al. 2013). A spherical morphology of Bio-Fe-NPs was also reported in previous studies as shown in Fig. S1c (Huo et al. 2016; Cutting et al. 2010).

The crystalline nature of biogenic Bio-Fe-NPs is usually characterized by an X-ray diffraction (XRD) analysis. Many studies found an amorphous or poorly crystalline structure of Bio-Fe-NPs, which usually shows weak diffraction peaks in XRD profiles (Bai et al. 2016; Huo et al. 2016; Pi et al. 2017). When comparing the XRD patterns, researchers noticed that the diffraction peaks of biogenic Fe (oxyhydr)oxides were quite broader than those of synthetic two-line ferrihydrite, indicating that the former may possess a more disordered structure (Whitaker et al. 2018). However, the crystalline of Bio-Fe-NPs can be highly influenced by many factors in biosynthesis including but not limited to the initial rate of Fe reduction, electron carriers, and excreted substances (Cutting et al. 2009). The appearance of lattice fringes in the TEM images has proved that the poorly ordered schwertmannite was transformed into a highly crystalline biogenic magnetite when incubated with *G. sulfurreducens* (Cutting et al. 2010). Further study suggested that the reduction of ferrihydrite was proceeded in 3 ~ 7-day incubation and stayed in a stable state after 7 days and finally formed a mixed-valent magnetite crystal ($Fe^{II}Fe^{III}_2O_4$) which contained low bioavailable Fe(III) for Fe(III)-reducing bacteria (Iwahori et al. 2014). In addition, with the assistance of surface-bound components, the non-magnetic akaganeite was transformed into metallic face-centered cubic magnetic precipitate by *Shewanella oneidensis* MR-1 under anaerobic conditions (Tuo et al. 2015).

Table 1 The main Bio-Me-NPs reported in literatures

Biogenic source		Types	Morphology	Size	Valence	Distribution	Refs
Bacteria	*Pseudomonas* sp. QJX-1	Fe oxide	Identical to lepidocrocite	330 nm	Mixed valency	–	Bai et al. 2016
	Pseudomonas sp. QJX-1	Fe–Mn oxides	Poor crystallinity	370 ~ 400 nm	Fe: mixed valency Mn: + IV		
	L. discoph ora SS-1	Fe(hydr)oxide	Amorphous or poorly crystallinity	–	+ III	Extracellular	Nelson et al. 2002
	Geobacter sulfurreducens	Nano-scale magnetite	–	~ 20 nm	–	–	Coker et al. 2014
	Shewanella oneidensis MR-1	Fe_3O_4	Metallic face-centered cubic Fe_3O_4	3 ~ 15 nm	Mixed valency	–	Tuo et al. 2015
	FBR iron-oxidizing community	Ferric precipitates	–	–	+ III	–	Ahoranta et al. 2016
	Geobacter-like organism	Magnetite	Magnetite crystal ($Fe^{II}Fe^{III}{}_2O_4$)	Less than a few tens nanometers	Mixed valency	–	Iwahori et al. 2014
	Shewanella putrefaciens CN32	Mackinawite	Crystalline mackinawite	–	+ II	–	Veeramani et al. 2013
	Shewanella putrefaciens CN32	FeS	Poor crystallinity	100 nm	+ II and III	–	Huo et al. 2016
	Geobacter sulfurreducens	Magnetite	Crystallinity	5 ~ 20 nm	0	–	Watts et al. 2015
	Geobacter sulfurreducens	Magnetite	High crystallinity	10 ~ 20 nm	+ II and III	–	Cutting et al. 2010
	Shewanella putrefaciens strain CN32	Magnetite	Crystallinity	10 nm	+ II and III	–	Veeramani et al. 2011
		Vivianite	Crystallinity	Submicron to micron range	+ II		
	Shewanella sp.	Fe oxide	Well crystallized	10.0 ± 4.0 nm	Mixed valency	Extracellular	Jung et al. 2008
	Marine microbial consortium	Mn particles	Amorphous	Micrometer-scale	+ II	–	Zhou et al. 2016
	Pseudomonas sp. QJX-1	Mn oxides	–	–	+ III ~ + IV	–	Bai et al. 2017
	Pseudomonas putida MnB6	Mn oxides	Poor crystallinity	–	+ II and IV	On cell wall	Forrez et al. 2010
	L. discophora SS-1	Mn (Hydr)oxides	Amorphous	–	+ III/IV	Extracellular	Nelson et al. 2002
	Leptothrix discophora SP-6	Mn oxides	Resembles todorokite	20 ~ 100 nm	+ 3.8 (average)	Extracellular	Kim et al. 2003
	*Brachybacterium sp.*strain Mn32	Mn oxides	Crystal structures of σ-MnO_2 and γ-MnOOH	0.7 mm	+ III/IV	Extracellular	Wang et al. 2009
	Pseudomonas sp. QJX-1	Mn oxides	Attributed to σ-MnO_2 or birnessite	700 ~ 800 nm	+ IV	–	Bai et al. 2016

Table 1 (continued)

Biogenic source		Types	Morphology	Size	Valence	Distribution	Refs
	Pseudomonas sp. G7	Mn oxides	Amorphous	–	+II, III, and IV	–	Tian et al. 2018
	Pseudomonas putida MnB-1	Mn oxides	Poorly crystalline	–	+IV	Extra and intracellular	Zhou et al. 2018
	S. putrefaciens CN-32 *S. loihica* PV-4	Mn oxides	Poorly crystalline	Nanosize	+IV	–	Wright et al. 2016
	Shewanella oneidensis	Pd particles	–	Nano-scale	0	–	Mertens et al. 2007
	C. butyricum and *C. braakii*	Pd particles	Crystalline Pd (0)	–	0	Extracellular	Hennebel et al. 2011
	Thalassospira sp., *Halomonas* sp., and *V. natriegens*	Pd particles	Corresponded to Pd (0) and PdO	5 ~ 10 nm	0 and + II	In cytoplasm and periplasmic space	Hosseinkhani et al. 2014
	Bacillus sp.			15 ~ 20 nm		In the periplasmic space and on the cell wall	
	C. *pasteurianum* BC1	Pd particles	Metallic and crystalline	11.8 ± 4.5 nm	0	On the cell wall and within the cytoplasm	Chidambaram et al. 2010
	Escherichia coli K12	Au particles	Single-crystalline	50 nm	0	–	Srivastava et al. 2013
	Actinomycete *Gordonia amicalis* HS-11	Au particles	Metallic gold crystals	–	0	Extracellular	Sowani et al. 2016
		Ag particles	Metallic silver crystals	–	0	Extracellular	
	Shewanella oneidensis MR-1	Au particles	Au (0)-crystals	5 ~ 10 nm	0	Mostly intracellular	De Corte et al. 2011b
	Enterobacteria	Ag particles	Metallic Ag nanocrystallites	52.5 nm	0 and + I	–	Shahverdi et al. 2007
	Lactobacillus fermentum	Ag particles	–	11.2 ± 0.9 nm	0	On the cell wall	Sintubin et al. 2011
Fungi	*Penicillium oxalicum*	Ag particles	Highly crystalline	11 nm	–	–	Du et al. 2015
	Pleosporales sp. Y-5	Mn oxides	Poorly crystalline	9.6 nm	+IV	–	Xie et al. 2018
	Acremonium strictum strain KR21-2	Mn oxides	Analogously to vernadite	–	–	–	Zheng et al. 2016
	Strain KR21–2	Mn oxides	Poorly crystalline	–	–	Associated with hyphae	Tani et al. 2004
	Acremonium sp. strain KR21-2	Mn oxides	Poorly crystalline	–	–	–	Tanaka et al. 2010
Algae	Desmodesmus sp. *WR1*	Mn oxides	Amorphous	Nanosize	+III	Extracellular	Wang et al. 2017
	Chlamydomonas reinhardtii	Ag particles	Highly crystalline	5–40 nm	0	Extra and intracellular	Barwal et al. 2011
	Chlorella pyrenoidosa	Ag particles	Face-centered cubic	8 ± 2 nm	0	–	Aziz et al. 2015
	Scenedesmus sp.	Ag particles	Spherical crystalline	15–20 nm	0	Intracellular	Jena et al. 2014

Table 1 (continued)

Biogenic source	Types	Morphology	Size	Valence	Distribution	Refs
Pithophora oedogonia	Ag particles	Cubical and hexagonal-shaped	34.03 nm	0	Extracellular	Kathiraven et al. 2015
Ecklonia cava	Au particles	Face-centered cubic	30 ± 0.25 nm	0	Extracellular	Venkatesan et al. 2014
Others –	Fe (oxyhydr) oxides	–	–	+ III	–	Whitaker et al. 2018
–	Fe sulfides	Poorly crystalline phase	–	+ II	–	Pi et al. 2017
Granular biomass	Pd particles	Cubic crystal planes of metallic Pd	4.78 nm	0	On the surface	Suja et al. 2014

Bio-Mn-NPs

The oxidation of Mn in the natural environment is mainly attributed to the microbes since the rate of microbial oxidation of Mn(II) to Mn(III/IV) is several orders of magnitude (up to 10^5 times) higher than that of abiotic oxidation (Furgal et al. 2015; Tanaka et al. 2010). Bio-Mn-NPs acquire non-uniform crystallines in different cases. Amorphous structured or poorly crystalline Bio-Mn-NPs (represented by Fig. S2) exist prevalently as mentioned in previous studies (Tanaka et al. 2010; Tian et al. 2018; Wang et al. 2017; Zhou et al. 2018). As indicated by the XRD patterns, plenty of Bio-Mn-NPs were of poor crystallinity and analogously to natural minerals including birnessite (σ-MnO_2), manganite (γ-MnOOH), todorokite, and vernadite (Kim et al. 2003; Wang et al. 2009; Xie et al. 2018; Zheng et al. 2016). For instance, the final products in biogenic Mn(II) transformation processes were reported as a mixture of rhodochrosite ($MnCO_3$), sidorenkite [$Na_3Mn(PO_4)(CO_3)$], and amorphous manganese oxides (Zhou et al. 2016). The well crystal structured Bio-Mn-NP has been also reported. Bio-Mn-NPs produced with *Pseudomonas* sp. QJX-1 were comprised of discrete layered σ-MnO_2 or birnessite with adjacent layers randomly stacked (Bai et al. 2016). Another research found that Bio-Mn-NPs with diffraction peaks at 36.4°, 38.2°, 43.2°, 53.2°, 26.5°, 33.4°, and 38.8° 2θ were ascribed to birnessite and γ-MnOOH (Wang et al. 2009). Actually, the highly crystalline biogenic NPs was reduced at lower rate than amorphous, disordered one since poor crystallinity characterized by greater surface area and structural defects was beneficial to electrons transfer (Wright et al. 2016).

The Mn valence of Bio-Mn-NPs can fluctuate from + II to + IV, largely depending on the reduction capacity of biogenic source and the species of substrate. The main valence state of Bio-Mn-NPs with *P. putida* MnB-1 was found to be + IV, as demonstrated by XPS analysis (Zhou et al. 2018). Mixed Mn valences such as co-existence of + II and IV or + II, III, and IV, were also frequently detected in previous studies (Du et al. 2020; Nelson et al. 2002; Tian et al. 2018; Wang et al. 2009).

Bio-Pd-NPs

With electron donors supplied, the bioreduction of Pd(II) can proceed through a metabolic activity. Pd may precipitate on cell surface, debris, periplasmic, cytoplasm, or independently from biomass (Hennebel et al. 2011). Baharak et al. isolated several marine strains with the ability to generate Bio-Pd-NPs, including both Gram-negative and Gram-positive strains (Hosseinkhani et al. 2014). They also found that Bio-Pd-NPs were located in the cytoplasm and periplasmic space of the Gram-negative strains while in the periplasmic space and on the cell wall of Gram-positive strains (shown in

Fig. S3). The thinner peptidoglycan layer of Gram-negative bacteria can be favorable for transferring Pd(II) to the cytoplasm, consequently leading to an intracellular precipitation. The precipitation profile was found to be determined by metabolic activities of cells and the electron donor for bioreduction. For instance, smaller and more Pd(0) particles were distributed on the cell surface and inside the periplasm when comparing H_2 with formate as electron donors (Windt et al. 2005).

XRD patterns and TEM analysis indicated that Bio-Pd-NP is metallic crystalline in nano-sizes. Bio-Pd-NP production with an indigenous marine bacterial community was manifested as the conversion from Pd(II) ions to metallic Pd(0) and PdO crystals (Hosseinkhani et al. 2014). A cubic crystal metallic Bio-Pd-NP was generated by microbial granules using bio-H_2 as electron donor (Suja et al. 2014). Researchers also found that Bio-Pd-NPs produced by both *C. pasteurianum* BC1 and *Citrobacter braakii* were in metallic and crystalline phase after a 2-week successive cultivation (Chidambaram et al. 2010; Hennebel et al. 2011).

Bio-Au and Ag-NPs

Bio-Au and Ag-NPs were found to be associated with the cells or precipitated intracellularly which corresponds to the distribution of other Bio-Me-NPs aforementioned (Binoj and Pradeep 2002; Du et al. 2015). Bioreduction of Au and Ag is prone to form well crystalline NPs. Bio-Au and Ag-NPs derived from the Actinomycete *Gordonia amicalis* HS-11 were depicted with a face-centered cubic (fcc) crystalline (Sowani et al. 2016). Another study also found in the TEM images of Ag nanocrystallites two areas consisting of silver NPs and micro crystalline insoluble Ag salts, respectively (Shahverdi et al. 2007). Biomolecules can largely influence the morphology of Bio-Me-NPs especially in the control of shapes. Zhang et al. (2016) reported that Bio-Au-NPs synthesized by the strain LH-F1 exhibited various sizes and shapes including triangle, hexagon, pentagon, and irregular shapes (Fig. S4), whereas Bio-Au-NPs originated from *Escherichia coli* K12 were strictly controlled in the circular shape of approximately 50 nm with the aid of stabilizing agents (Srivastava et al. 2013).

Bio-bimetal-NPs

Dosing two kinds of metals in the substrate solution may form the biogenic bimetal NPs, which can enhance the activity of NPs due to the change in geometric and physicochemical properties (De Corte et al. 2011a; Nutt et al. 2005). Fe and Mn elements commonly co-exist in terrestrial and aquatic environments (Huang et al. 2012). Bai et al. (2017) obtained Bio-Fe/Mn-NPs with a strong adsorption capacity of As ions, and the size of Bio-Fe/Mn-NPs was between Bio-Mn-NPs and Bio-Fe-NPs generated under similar conditions. Another study found with XRD and EDX analysis that Bio-Fe/Mn-NPs were not homogenous and showed a poor crystalline (Bai et al. 2016). De Corte et al. also found that Bio-Pd/Au-NPs (seen in Fig. S5) produced by means of decorating Au particles on Bio-Pd-NPs can improve the removal of halogenated organics (De Corte et al. 2011a, 2012).

Composite Bio-Me-NPs

In order to enhance the stability, to avoid the agglomeration, to protect from poisoning, and to reduce metal ions leaching into environment as well, one can immobilize or encapsulate Bio-Me-NPs as composite materials (Parshetti & Doong 2008). Hennebel et al. (2010) immobilized Bio-Pd-NPs on polysulfone membranes in a fed batch configuration and obtained 77% removal efficiency for 20 ppm of diatrizoate within 48 h. Another work of Hennebel et al. (2009c) eliminated 98% trichloroethylene in 22 h by polyurethane cubes empowered with bio-Pd-NPs. Moreover, biogenic jarosite composited with TiO_2 via Fe–O–Ti bonds possessed stronger charge transfer capacity in photocatalytic degradation of methyl orange, and the electrical energy consumption derived from artificial light was 4 times lower than that of pristine P25 (Chowdhury et al. 2017). The photoelectrochemical property of Bio-Au-NPs decorated on polymeric graphitic carbon nitride (g-C_3N_4) as shown in Fig. S6 was strengthened as a result of the synergistic effects between the conduction band of g-C_3N_4 and the plasmonic band of AuNPs (Khan et al. 2018). In general, the composite strategy compensates for the shortcomings of Bio-Me-NPs and provides more potentials for its further application.

Biosynthesis of metal NPs

The participation of toxic and costly substances in conventional chemical synthesis of NPs may pose potential threats to human and environmental health. Biosynthesis of NPs with microbes such as bacteria, fungi, and algae through bioaccumulation, precipitation, biomineralization, and biosorption is becoming an attractive alternative (Srivastava et al. 2013). When an applicable concentration of metal ions exists, certain amount of them will be transferred into cells through the endocytosis, the carrier-mediated transport, and the permeation process (Issazade et.al, 2013). Microbes may excrete some enzymes which can mediate the intracellular and extracellular transformation of metals ((Parandhaman

et al. 2019). Herein, the processes of biosynthesis with different microbes are discussed below.

Bacteria

Bacterial transformation of metals plays a pivotal role in geochemical cycles of many elements. Many strains of bacteria can mediate the metal transformation and obtain energy for its metabolism process. The organics can serve as reductive and stabilizing agents during the synthesis of Bio-Me-NPs and promote the interaction between NPs and pollutants (Zhou et al. 2016). The transformation of metals by bacteria is also regarded as a detoxification mechanism of metals, reactive species, and other substances that are toxic to cells (Tebo et al. 2005; Kim et al. 2003).

The process of Au NPs synthesized by *Shewanella oneidensis* was described as a rapid biosorption firstly and a slow reduction process in the second stage (De Corte et al. 2011b). For the generation of biogenic Fe NPs, a conspicuous color distinction with different Fe source was detected (Furgal et al. 2015; Wright et al. 2016). Bio-Fe-NPs derived by *S. putrefaciens* CN32 with hydrous ferric oxide as precursor resulted in a black precipitate, whereas a grayish white precipitate was displayed with Fe(III)-citrate as precursor, which were further verified as magnetite and vivianite, respectively (Veeramani et al. 2011).

The transformation of Mn(II) can be realized by many manganese-oxidizing bacteria (MnOB) like *Pseudomonas putida* MnB-1, which can utilize Mn(II) to consume superoxides for self-protection (Zhou et al. 2018). The formation of Bio-Mn-NPs mainly include two steps: (1) Mn(II) is firstly oxidized to an intermediate of Mn(III), which is confirmed by studies with sodium pyrophosphate as a trapping reagent; (2) the formed Mn(III) intermediate is further oxidized to MnOx (Spiro et al. 2010; Tran et al. 2018). The organic pollutants in the aquatic environment can be adsorbed and degraded by the biogenic MnOx (Bio-MnOx), concomitantly releasing oxidative products and Mn(II) ions that can be re-oxidized by *Pseudomonas putida* MnB-1 (Forrez et al. 2009). In this process, enzymes like multicopper oxidases and peroxidases were requisite actuating force for metal oxidation (Andeer et al. 2015; Zhang et al. 2015b). With the assistance of Mn-oxidizing bacteria, Bio-MnOx has the potential to be regenerated consecutively, which is of great significance in the practical application in water remediation (Furgal et al. 2015).

Fungi

Fungi are well known as "the nanofactory" for its high tolerance to many metals in Bio-Me-NP production (Balaji et al. 2009; Shahverdi et al. 2007). In the biosynthesis of Bio-MnOx produced by fungus strain KR21-2, the fungal hyphae was found to be the main region for Bio-MnOx formation and the optimal concentration of Mn(II) as precursor was up to 1.2 mM (Tani et al. 2004). Instead of exogenous chemicals, biomolecules are deemed to be the prerequisite for the formation and stabilization of NPs. Du et al. stated that fungus *Penicillium oxalicum* was able to reduce Ag ions to highly crystalline Ag NPs with the characteristics of high stability and great dispersion (Du et al. 2015, 2011). With the assistance of capping agents secreted by fungi, Bio-Au-NPs produced by *Magnusiomyces ingens* LH-F1 showed a high dispersity (Das et al. 2010; Gangula et al. 2011; Zhang et al. 2016). In the case of Fe NPs generated by *Fusarium oxysporum*, the biomolecules worked as stabilizing agents to control the shape and size of the formed crystalline magnetite (Bharde et al. 2006).

Algae

Another clean and sustainable microbial route for the biosynthesis of metal NPs is algae. It has been found that algae can transfer metals such as Ag, Mn, Cu, and Au into Bio-Me-NPs (Abboud et al. 2013; Kathiraven et al. 2015; Prasad et al. 2012; Venkatesan et al. 2014). In the photosynthesis process, algae *Desmodesmus* sp.WR1. can increase the level of pH and dissolved oxygen (DO) by consuming CO_2 and consequently expedite the oxidation of Mn^{2+} to form Bio-Mn-NPs (Wang et al. 2017). Shankar et al. (2016) explained the three stages in biosynthesis of Ag and Au as follows: (1) Ag or Au ions were reduced and formed nucleus; (2) then, small particles aggregated into larger one and the molecular stability was established to a certain extent; (3) the formation of NPs in different shapes took place in the final stage. Similar to the microbes mentioned above, extracellular and intracellular enzymatic reductions contribute largely in this process (Barwal et al. 2011; Jena et al. 2014). The enzymes can also significantly influence the morphology of generated Me-NPs (Aziz et al. 2015). For example, Ag^+ reduction mediated by ATP synthase, superoxide dismutase, carbonic anhydrase, ferredoxin-NADP + reductase, etc. formed rounded or rectangular Ag NP intracellular (Barwal et al. 2011). As documented by Xie et al. (2007), Au was reduced by enzymes derived from algae and the single-crystalline NP was in the form of triangular and hexagonal shapes. Likewise, the high consistency of Bio-Ag-NPs produced by *chlorella pyrenoidosa* was attributed to the morphology control effects of a large amount of enzymes and proteins (Aziz et al. 2015). Additionally, hydroxyl, carboxyl, and amino functional groups on the surface of biomolecules can promote the adsorption of metal ions by electrostatic interaction and further serve as reducing and capping agents (Mahdavi et al. 2013).

As shown above, researchers have demonstrated the capacity of bacteria, fungi, and algae to generate Me-NPs.

However, studies have not been conducted to evaluate the applicability of the microbes for a large-scale synthesis of Bio-Me-NPs. Bacteria might be a potential candidate for the scale-up due to their wide variety of strains and high yield efficiency. Algae may find a unique position when the CO_2 immobilization is considered. The application of fungi is faced with the challenge of long-term stability due to the problems like microbial contaminations, strict nutrient conditions, and reproduction.

Applications of biogenic metal NPs in water treatment

The migration of heavy metals, textile dyes, pesticides, pharmaceuticals, and personal care products in environment causes severe pollution, which may bring potential threats to the human health once entering the food chain (Lingamdinne et al. 2017; Martins et al. 2017; Mertens et al. 2007; Muthukumar et al. 2017; Qu et al. 2017). Although being detected in low concentrations in water body, these compounds may impose detrimental effects on digestive, immune, and reproductive systems of human (Roberts et al. 2016; Zhang et al. 2003). Due to some special characteristics such as large specific surface areas, weak crystalline, and complex valence, Bio-Me-NPs have been studied to eliminate various pollutants via the mechanisms of adsorption, oxidation, reduction, and catalysis, which is outlined in Table 2.

Adsorption

The large specific area, wide valent distribution, and unique structure of Bio-Me-NPs attract a lot of research efforts in adsorption (Fig. 1). A wide range of metal ions including Cu(II), Fe(III), Pb(II), Zn(II), and U(VI) can be effectively adsorbed by Bio-Mn-NPs owing to its large surface area with negative charges (Spiro et al. 2010; Zhou et al. 2016). Wang et al. (2009) reported the superior adsorption of heavy metals by Bio-MnOx. With the dosage of Mn oxides as 0.1 mM and the concentration of heavy metals as 30 μM, the adsorption of Zn(II) and Ni(II) of Bio-MnOx is 2 ~ 3 times higher than that of commercial and abotic MnO_2. The XRD patterns revealed that the biogenic one contained crystalline birnessite with a high specific area and a cation-exchange capacity, which possibly accounted for its extraordinary adsorption of metals (Wang et al. 2009). It was also found that the Pb binding ability of Bio-MnOx was much higher than that of abotic Mn-bearing materials, suggesting a stronger binding energy per unit surface area of the former (Nelson et al. 2002).

Notably, a recent study showed that the surface charge of adsorbates may strongly impact the adsorption performance (Bai et al. 2017). In the study, Sb(III) was effectively adsorbed but the adsorption abated after Sb(III) was oxidized into Sb(V). Though the negatively charged Bio-MnOx rejected both Sb(III) and Sb(V) (existing as negatively charged groups), the binding force between Sb(III) and MnOx was higher than the charge repulsion and finally the stable ligand between $Sb(OH)_3$ and Bio-MnOx was formed through the inner-sphere electron transfer.

The distinct structural property works potently as well. The intrinsic structural defects in Bio-MnOx can provide vacancies for metals and thus can promote the combination of metal cation ions on Bio-MnOx (Cao et al. 2015). Previous studies mentioned that Pb–Mn complexes in triple-corner-sharing inner-sphere surface and double-edge-sharing Pb(II) inner sphere surface were relevant to O ions with unsaturated bonds (Takahashi et al. 2007; Villalobos et al. 2005). Consistent results revealed that octahedral FeO_6 composition in the biogenic particles could lead to the strong adsorption of As(III and V) (Bai et al. 2016). Pi et. al. (2017) elaborated that the removal of As by Bio-Fe NPs was due to the adsorption on the surface at first and then co-precipitation as a stable As–Fe complex (Pi et al. 2017). Aside from metal ions, Bio-Me-NPs can also adsorb phosphorus and many other organic contaminants which are often followed with oxidation or reduction as discussed below (Rentz et al. 2009; Zhou et al. 2016).

Oxidation

Some metals in Bio-Me-NPs hold a high valence and thus could exhibit a certain level of oxidation potential. Bio-MnOx, as a widely studied example, is able to oxidize many recalcitrant pollutants like benzophenone-4, estrone, and 17-α-ethinylestradiol (EE2) due to the existence of highly valency Mn (close to IV) (Chang et al. 2018; Furgal et al. 2015). Despite the extensive researches of chemically synthetic Mn(IV)-containing materials, Bio-Mn-NPs show several superior properties.

Large specific area facilitates many interactions. For example, in the work of Forrez et al. (2010), diclofenac was chosen as a model contaminant at initial concentration of 4 mg/L and the dosage of chemical MnO_2 and Bio-MnOx is 4.6 vs. 3.5 mg Mn^{4+} L^{-1}, respectively. The enhanced diclofenac oxidation by Bio-Mn-NPs was attributed to the relatively larger specific surface area than the chemical synthesized MnO_2 (98–224 m^2 g^{-1} vs 58–121 m^2 g^{-1}) (Forrez et al. 2010). Low crystallinity with more structural defects may be another enhancement factor. Extended X-ray absorption fine structure spectroscopy (EXAFS) indicated that Bio-Mn-NPs held massive Mn(IV) vacancy sites which can provide binding sites for exogenous ions (Spiro et al. 2010). It has been reported that amorphous structure of Bio-Mn-NPs was conducive to surface electron transfer for the oxidation of α-ethinylestradiol (Tran et al. 2018). In Mn^{2+}-enriched

Table 2 The application of biogenic nanoparticles in wastewater treatment

Metal species	Applications		Mechanisms	Refs
	Pollutants	Activity		
FeS	30 μM CCl_4	100%, 10 h, 0.35 h^{-1}	Reduction	Huo et al. 2016
Fe	20 mM TcO_4	6.98 h^{-1}	Reduction	Fredrickson et al. 2004
Fe	0.96 mM Cr(VI)	50%, 14 days	Reduction	Whitaker et al. 2018
Mn	2.0 μM Pb	550 mM of Pb/M of Mn	Adsorption	Nelson et al. 2002
Magnetite	12 μM Zn^{2+}, 13 μM Ni^{2+}, 15 μM Co^{2+}, and 18 μM Mn^{2+}	26, 24, 27, and 66 mM Co, Ni, Mn, and Zn/M of Fe	Adsorption	Iwahori et al. 2014
Iron oxides	1.3 mg/L P	0.165 ± 0.037 h^{-1}	Adsorption	Rentz et al. 2009
Fe–Mn	10 μM As(III)	> 80%,72 h	Fe: adsorption Mn: oxidation	Bai et al. 2016
Fe–Mn	10 μM Sb	0.033 mg Sb/mg total Fe + Mn	Fe: adsorption Mn: oxidation	Bai et al. 2017
Jarosite	100 mg/L As	99.5%, 48 h	Adsorption + co-precipitation	Ahoranta et al. 2016
FeS	593 mg/L As	77%, 30 days	Adsorption + co-precipitation	Pi et al. 2017
Au	0.1 mM 4-nitrophenol	100%, 10 min; 1.24×10^{-2} min^{-1}	Catalysis	Srivastava et al. 2013
Au	0.1 mM nitrophenols	100%, 5 min; 13.8 ~ 32.5 s^{-1}	Catalysis	Zhang et al. 2016
Pd-Au	20 mg/L diclofenac and 100 mg/L trichlorethylene	1.554 and 0.078 ($Lh^{-1}g_{Pd}^{-1}$)	Catalysis	De Corte et al. 2011a
Ag	200 mM methylene blue	–	Catalysis	Du et al. 2015
Bio-Pd/Au	6.4 mg L^{-1} diclofenac	48%, 24 h; 0.52 h^{-1}	Catalysis	De Corte et al. 2012
Pd	2 mg L^{-1} diatrizoate	85%, 24 h	Catalysis	De Gusseme et al. 2011
Pd	10 mg/L lindane	98%, 24 h	Catalysis	Mertens et al. 2007
Pd	100 mg/L trichloroethylene	2515 mg day^{-1} g^{-1} Pd	Catalysis	Hennebel et al. 2009b
Pd	1 mg/L polychlorinated biphenyl	90%, 5 h	Catalysis	Windt et al. 2005
Pd	20 mg L^{-1} trichloroethylene	100%, 1 h	Catalysis	Hosseinkhani et al. 2014
Biomass + Pd	0.25 mM P-nitrophenol and Cr (VI)	100%, 1 h (P-nitrophenol); 100%, 24 h (Cr)	Catalysis	Suja et al. 2014
Biomass + Pd	26 mg L^{-1} Cr(VI)	45% (10 min) and 72% (72 h)	Catalysis	Chidambaram et al. 2010
Mn	10 mg/L Co(II) and Ni(II)	53% (Co) and 19% (Ni), 50 days	Adsorption	Matsushita et al. 2018
Mn	30 μM Zn(II) and Ni(II)	85.5%, 4 days (Zn) 54.8%, 2 days (Ni)	Adsorption	Wang et al. 2009
Mn	15 μM Co(II), Ni(II), Zn(II)	99.2% (Co), 65.5% (Ni), 86.3% (Zn)	Adsorption	Tani et al. 2004
Mn	2.5 mg L^{-1} Ni(II) and Co(II) in influent	1.7 and 7.9 g m^3 day^{-1}	Adsorption	Cao et al. 2015
Mn	20 mg L^{-1} methylene blue	20.8 mg g^{-1}	Adsorption	Zhou et al. 2016
Mn	Environmentally relevant concentrations (ng mg L^{-1})	Ibuprofen (> 95%), naproxen (> 95%), diuron (> 94%), codeine (> 93%), N-acetyl-sulfamethoxazole (92%), chlorophene (> 89%), diclofenac (86%), mecoprop (81%), triclosan (> 78%), clarithromycin, (75%), iohexol (72%), iopromide (68%), iomeprol (63%), and sulfamethoxazole (52%) in MBR	Adsorption + oxidation	Forrez et al. 2011
Mn	13.5 mg L^{-1} bisphenol A	78%, 7 days	Oxidation	Wang et al. 2017
Mn	10 μg L^{-1} 17-a ethinylestradiol	100%, 5 days	Oxidation	Furgal et al. 2015
Mn	3 mg L^{-1} diclofenac	0.028 h^{-1}	Oxidation	Forrez et al. 2010
Mn	50 mg L^{-1} diclofenac	100%, 30 min; 0.28 min^{-1}	Oxidation	Xie et al. 2018

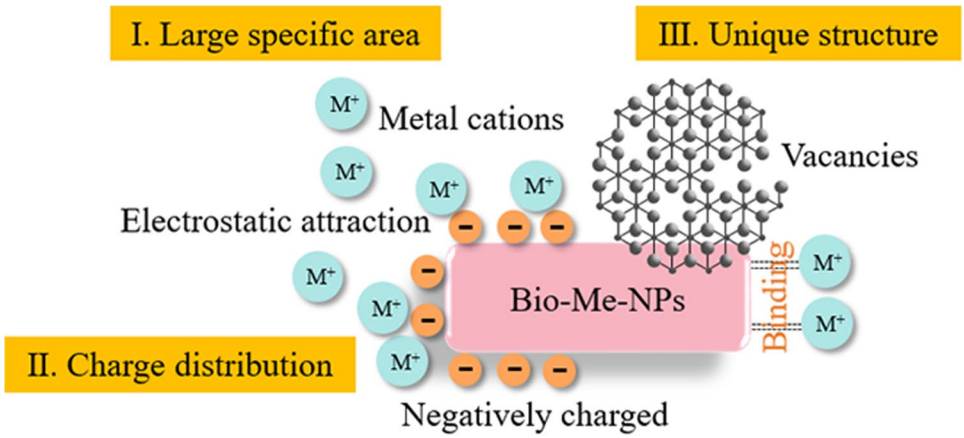

Fig. 1 Bio-Me-NPs mediated adsorption process

cultures, amorphous Bio-Mn-NPs was formed and increased the removal efficiency of bisphenol A by up to 51% (Wang et al. 2017). With the existence of microbes, Bio-Mn-NPs further exerts its superiority. A recent study systematically depicted the ciprofloxacin (CIP) degradation in a Mn redox cycling system (Zhou et al. 2018). As portrayed in Fig. 2, *Pseudomonas* putida MnB-1 generated Bio-MnOx in two steps through Mn(III) intermediates (Spiro et al. 2010). Both Bio-MnOx and Mn(III) intermediates contributed to the oxidation of CIP; however, Mn(III) intermediates survive only in a short time (Tran et al. 2018). The resulting Mn^{2+} was detrimental to the oxidation of CIP by blocking the active sites on the surface of Bio-MnOx (Watanabe et al. 2013). The re-oxidation of Mn^{2+} by bioactivities can eliminate this negative effect, which is also crucial to the microbial redox cycle of Mn (Bai et al. 2016; Forrez et al. 2010). Re-oxidation of Mn^{2+} decreases the Mn(II) binding on the surface of Bio-MnOx and the process is influenced by DO content, pH, and oxidoreductases (Wang et al. 2017). Similar results were also obtained with the Fe–Mn oxides which can also release

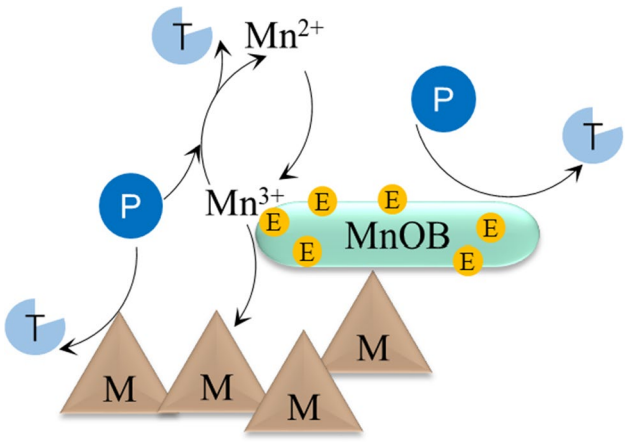

Fig. 2 Microbial Mn redox cycle. P stands for pollutants; T for transformation products; M for Bio-MnOx; E for enzymes; MnOB for manganese oxidizing bacteria

synthetic Fe and Mn ions which hinder the further activity (Bai et al. 2017, 2016).

Reduction

Bio-Fe-NPs own an appreciable reductive ability as well. A previous study reported that after being activated by *Shewanella alga* BrY, the inert ferric oxide was converted into microbial-produced Fe(II) that was capable of reducing 66% of Cr(VI) within 5 min (Vázquez-Morillas et al. 2006). The direct and indirect reduction processes conducted with Bio-Me-NPs are illustrated in Fig. 3. Compared with reactions conducted in pasteurized solution, the reduction of U(VI) by biogenic magnetite and vivianite was suggested as abiotic processes (Veeramani et al. 2011). Lu et al. studied the removal of nitrite through the microbial mediated iron redox cycling and found that both biotic and abiotic reduction occurred concurrently in the removal of nitrite (Lu et al. 2017). Coker et al. (2014) designed a hybrid system by associating hollow-fiber membrane with biogenic Pd-magnetite and achieved considerable removal of azo dye and Cr(VI). Besides the reduction capacity of Fe(II) in magnetite, Pd was able to scavenge electrons and thus to reduce the contaminant or to regenerate Fe(II). Moreover, it is worth mentioning that microbes can act as electron carriers and fix the charged reactants on an appropriate position to promote the reduction corporately (Kondo et al. 2015; Vázquez-Morillas et al. 2006). Some Bio-Fe-NPs may contain S^{2-}, like biogenic minerals such as mackinawite, pyrite, and marcasite. Veeramani et al. (2013) found that the sulfide in biogenic Mackinawite could initiate the reduction of U(VI), whereas Fe(II) in the NPs worked inertly in the process. The contribution of both Fe(II) and disulfide of biogenic FeS in dechloriantion process was also confirmed in another research (Huo et al. 2016). The promoted dechlorination by adsorbed Fe(II) was found

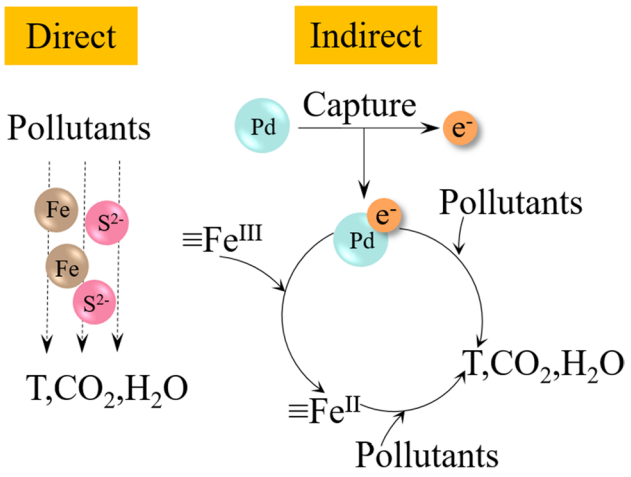

Fig. 3 Reduction process with different components in Bio-Me-NPs

previously, whereas a negative effect existed when Fe(II) was excessive (Huo et al. 2016). Other ions such as Ca, Si, and S may impair the reduction process by clogging the combination access (Roberts et al. 2004; Watts et al. 2015). The DO level in water can inhibit the reduction of Cr(VI) by competing the active site and finally oxidizing Fe(II) and Fe(0) (Watts et al. 2015). On the contrary, sulfate and carbonate can promote the reaction by precipitating as green rust that is conductive to electron transfer (Vázquez-Morillas et al. 2006).

Catalysis

The facile and benign route of Bio-Me-NPs synthesis makes it a promising method to generate catalysts with microbes and without involving toxic solvents and complex operations (Fig. 4). Some special characteristics also enable Bio-Me-NPs a higher catalytic performance than the chemically synthesized peers (Jung et al. 2008).

The most extensively studied issue is the catalytic reduction ability, in which exogenous reductants like $NaBH_4$, H_2, and formate and formic acid are often added to serve as electron donors (Hennebel et al. 2009b; Srinath & Ravishankar Rai 2015; Tuo et al. 2015). With Bio-Au-NPs as a catalyst, MB can be reduced to methylene blue by $NaBH_4$ (Srinath & Ravishankar Rai 2015; Suvith & Philip 2014). Hennebel et al. (2009b) found in the catalytic TCE dechlorination with Bio-Pd-NPs that a rapid process involving radicals was initiated when formic acid was applied as a hydrogen donor, whereas a slow hydride formation process was dominated instead when formate was used as a hydrogen donor. H_2 produced by microbes under fermentative conditions can be an

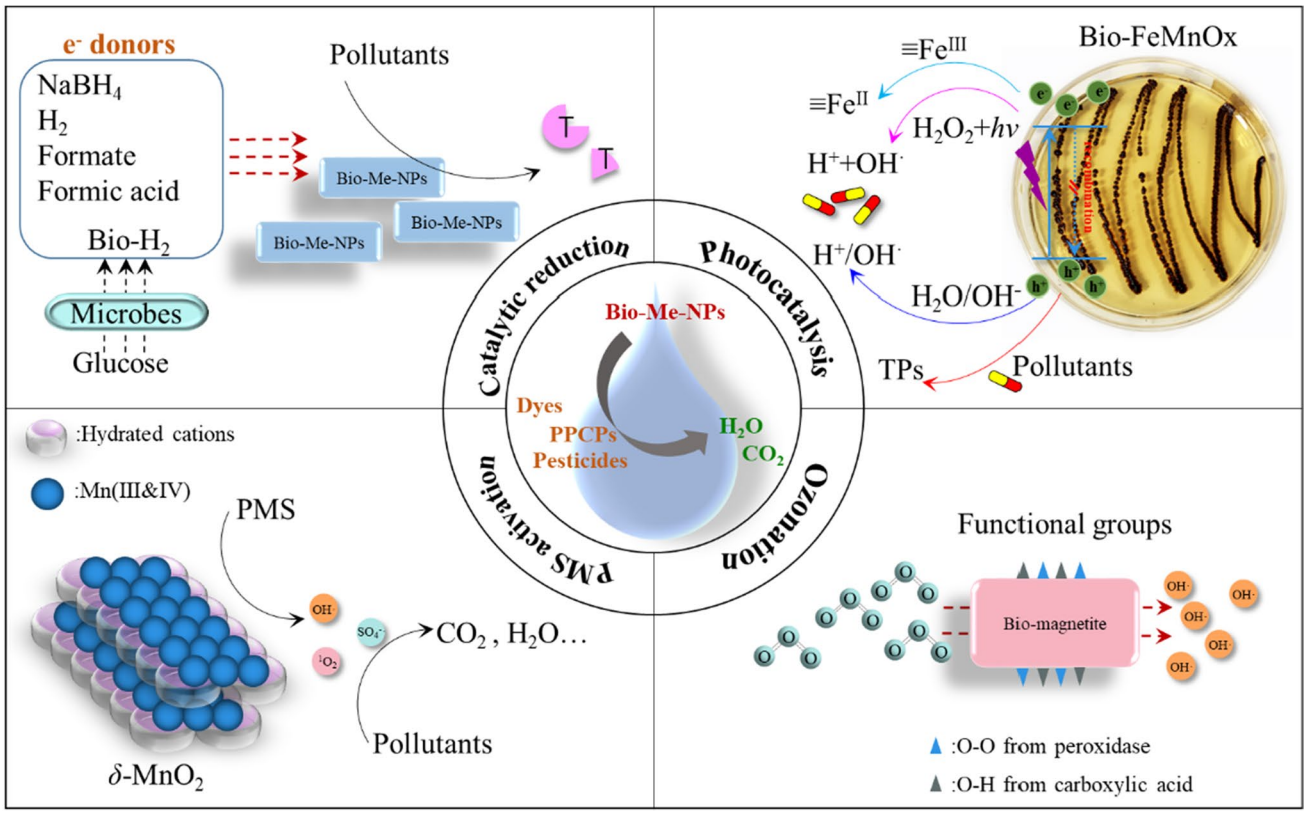

Fig. 4 Catalysis with Bio-Me-NPs

excellent alternative to exogenous reducing agents owing to its effective and economical production route (Chidambaram et al. 2010; De Gusseme et al. 2011; Hennebel et al. 2011; Hosseinkhani et al. 2014; Suja et al. 2014). Biocatalysts can be charged by in situ biogenic H_2 derived from the oxidation of glucose, which in turn facilitates the production of H_2 (Hosseinkhani et al. 2014). Under this circumstance, more than 90% removal of iomeprol, iopromide, and diatrizoate at environmentally relevant concentrations was obtained (Forrez et al. 2011). Except for H_2, Bio-Pd-NPs can enhance the removal of Cr(VI) and azo dye by scavenging electrons for generating reductive Fe(II) species or reacting with pollutants directly (Coker et al. 2014). The attachment of noble metal Au on Pd onto biocatalysts can promote the catalytic activity due to the geometric effect that the lattice is constricted to form an optimal intermolecular distance and also due to the electronic effect that Au withdraws the electron density from Pd (De Corte et al. 2011a; Tuo et al. 2015). The catalytic ability of bimetallic bio-Pd/Au has been proved to work in the treatment of hospital wastewater containing diclofenac at neutral and alkaline pH (De Corte et al. 2012).

Recently, Bio-Me-NPs applied in AOPs gain growing interest of research. For instance, the bio-FeMnOx derived from *Pseudomonas* sp. exhibited a twofold higher catalytic activity in the photo-Fenton degradation of ofloxacin than that of chemically synthesized Fe–Mn oxides (Du et al. 2020). Sunlight-driven photocatalytic decolonization of dyes including congo red, malachite green, direct blue-1, and reactive black-5 was successfully carried out with Bio-Cu-NPs produced by *Escherichia* sp. SINT7 (Noman et al. 2020). It has been demonstrated that the surface functional groups of the biogenic magnetite enabled its feasible catalytic activity in ozonation as well (Jung et al. 2008). Moreover, the application of Bio-Me-NPs in the activation of peroxymonosulfate (PMS) was also reported, for the degradation of 30 mg/L phenol or 10 mg/L tetracycline with the dosage of the catalyst and PMS as 0.4 and 1 g/L, respectively. The catalytic degradation ability of Bio-MnOx was three times higher in a wide range of pH (3.0 ~ 9.0) than the chemically prepared 3D α-Mn_2O_3 (Tian et al. 2018). Further study ascribed the enhanced performance to the unique crystal structure of Bio-MnOx, whose contents of Mn(III and IV) increased the generation of SO^{-}_{4}· and OH· radicals (Xie et al. 2018). The catalytic activity of Bio-MnOx could also be regenerated by heat treatment at 400 °C for 2 h, which eliminated the inhibition of substances on the surface (Xie et al. 2018).

Although Bio-Me-NPs exhibit appreciative properties as a catalyst, the deficiency of aggregation and the leaching of heavy metal ions also need much attention (Jung et al. 2008; Srivastava et al. 2013). Immobilization with appropriate matrix could be a good solution by providing a sturdy support (Srivastava et al. 2013). The strategy of encapsulating the catalysts with polymeric membranes like polyvinylidene fluoride and polysulfone membranes can prevent from poisoning and agglomeration (Hennebel et al. 2010; Parshetti & Doong 2008). De Gusseme et al. (2011) doped Bio-Pd-NPs on the cathode of a microbial electrolysis cell for the dehalogenation of diatrizoate and found that Pd nanoparticles can decrease the cathode overpotential and catalyze the dehalogenation with H_2 as an electron donor.

Scaling-up feasibility

Some research efforts have been made on the feasibility of applying Bio-Me-NPs in real applications. Conventionally, Bio-MnOx has been widely involved in the removal of metals from water. The popular reactor for the purpose is biofilter (Nishi et al. 2020; Nitzsche et al. 2015). Recently, researchers tend to apply Bio-Me-NPs to eliminate recalcitrant organics. Forrez et al. (2011) developed an MBR system by incorporating Bio-MnOx in the membrane modules and obtained an effective removal of many emerging contaminates from secondary effluents, such as naproxen (> 95%), morphine (60%), N-acetylsulfamethoxazole (92%), clarithromycin (60%), and diuron (90%). A similar MBR was also applied with Bio-Pd-NPs (Hennebel et al. 2009b, 2011). However, the MBR should overcome the limitation of incorporating large amount of Bio-Me-NPs and the possible

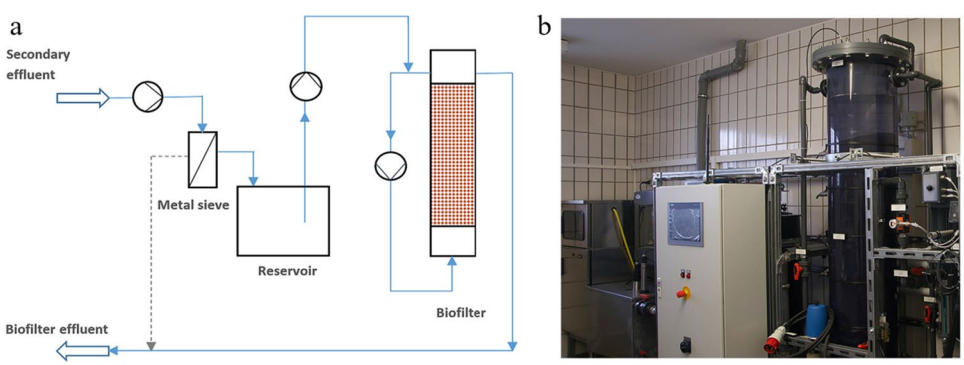

Fig. 5 The process scheme (**a**) and a photo (**b**) of the pilot biofilter. Reproduced from Zhang et al. (2017) with permission

membrane fouling issues coming from the direct contact of Bio-Me-NPs, which is still less concerned so far. Zhang et al. (2015a) operated a lab-scale aerated biofilter packed with natural MnOx and two strains of MnOB (*Leptothrix* sp. and *Pseudomonas* sp.) and obtained an effective removal of diclofenac and sulfamethoxazole in 1.5 years. Furthermore, they scaled up the biofilter to a pilot scale (250 L) which was installed at a local sewage treatment plants to treat the real secondary effluent and 70 ~ 98% of 15 emerging organic contaminants was eliminated in 500 days (Zhang et al. 2017). To our best knowledge, this reactor is still the largest one for the removal of recalcitrant organics with MnOB and the photo can be found in Fig. 5. This simple reactor worked effectively and continuously owing to the oxidation capacity of natural MnOx and the re-oxidation of Mn^{2+} by MnOB. However, the population analysis was not conducted so that the contribution of MnOB on the performance of biofilter is not clear. In addition, heterotrophic MnOB was incubated in a downflow hanging sponge reactor to produce Bio-MnOx, and Co and Ni ions in the effluent at an HRT in the range of 1.5–12 h were successfully removed after Bio-Mn-NPs formed (Cao et al. 2015). This reactor was able to remove Mn(II), Ni(II), and Co(II) simultaneously from wastewater in long-term continuous operation. In situ remediation is another promising strategy for groundwater treatment. Pi et al. (2017) injected $FeSO_4$ regularly into an As-contaminated aquifer at the central part of Datong Basin, China, for 25 days to motivate biogenic reduction and As was decreased by 73%, which was caused by surface-adsorption on and co-precipitation with formed biogenic Fe(II) sulfides.

Conclusions and outlook

The present work reviews the recent progress in the typical Bio-Me-NPs (Me = Fe, Mn, Pd, Au, or Ag) and their applications in water treatment. In general, the biosynthesis of Bio-Me-NPs with microbes like bacteria, fungi, and algae is environmentally friendly via avoiding toxic chemicals and extreme conditions. Bio-Me-NPs also possess some special characteristics, such as higher specific area, looser crystalline, more defects, and broader valence of metals, which could enable them a better performance in adsorption, oxidation/reduction, and catalysis than their chemically synthesized peers. The incorporation of multi-metals can further enhance the capacity of Bio-Me-NPs. Some efforts have also been made on the possible scale-up applications, such as with the reactor of MBR and biofilter.

However, there are still some issues waiting to be further clarified. For example, the performance of Bio-Me-NPs is strongly connected to their morphology whose regulation methods should be systematically studied. So far, most studies were conducted with a bench scale glassware in a batch mode and further efforts should be given on the continuous and long-term production of Bio-Me-NPs. Moreover, much work is needed to further explore the applicability of Bio-Me-NP in the water treatment at large scale.

Supplementary Information The online version contains supplementary material available at https://doi.org/10.1007/s11356-021-17042-z.

Author contribution Yongjun Zhang conceptualized the article and acquired the funding. Zhiling Du collected the literature and drafted the manuscript. Yunhai Zhang, Anlin Xu, Sunlong Pan, and Yongjun Zhang discussed the outline and critically revised the manuscript.

Funding The study is funded by the National Natural Science Foundation of China (grant no. 52070097), the Natural Science Research Program of Jiangsu Province for Colleges and Universities (grant no. 18KJA610001), and the Natural Science Foundation of Jiangsu Province (grant no. BK20200699).

Data availability Not applicable.

Declarations

Ethics approval and consent to participate Not applicable.

Consent for publication All the authors mutually agree for this submission.

Competing interests The authors declare no competing interests.

References

Abboud Y, Saffaj T, Chagraoui A, El Bouari A, Brouzi K, Tanane O, Ihssane B (2013) Biosynthesis, characterization and antimicrobial activity of copper oxide nanoparticles (CONPs) produced using brown alga extract (*Bifurcaria bifurcata*). Appl Nanosci 4(5):571–576

Ahoranta SH, Kokko ME, Papirio S, Özkaya B, Puhakka JA (2016) Arsenic removal from acidic solutions with biogenic ferric precipitates. J Hazard Mater 306:124–132

Andeer PF, Learman DR, McIlvin M, Dunn JA, Hansel CM (2015) Extracellular haem peroxidases mediate Mn(II) oxidation in a marine *Roseobacter bacterium* via superoxide production. Environ Microbiol 17(10):3925–3936

Aziz N, Faraz M, Pandey R, Shakir M, Fatma T, Varma A, Barman I, Prasad R (2015) Facile algae-derived route to biogenic silver nanoparticles: synthesis, antibacterial, and photocatalytic properties. Langmuir 31(42):11605–11612

Bai Y, Jefferson WA, Liang J, Yang T, Qu J (2017) Antimony oxidation and adsorption by in-situ formed biogenic Mn oxide and Fe-Mn oxides. J Environ Sci (china) 54:126–134

Bai Y, Yang T, Liang J, Qu J (2016) The role of biogenic Fe-Mn oxides formed in situ for arsenic oxidation and adsorption in aquatic ecosystems. Water Res 98:119–127

Balaji DS, Basavaraja S, Deshpande R, Mahesh DB, Prabhakar BK, Venkataraman A (2009) Extracellular biosynthesis of functionalized silver nanoparticles by strains of *Cladosporium cladosporioides* fungus. Colloid Surface B 68(1):88–92

Barwal I, Ranjan P, Kateriya S, Yadav SC (2011) Cellular oxidoreductive proteins of *Chlamydomonas reinhardtii* control the biosynthesis of silver nanoparticles. J Nanobiotechnol 9:1–12

Bharde A, Rautaray D, Bansal V, Ahmad A, Sarkar I, Yusuf SM, Sanyal M, Sastry M (2006) Extracellular biosynthesis of magnetite using fungi. Small 2(1):135–141

Binoj N, Pradeep T (2002) Coalescence of nanoclusters and formation of submicron crystallites assisted by *Lactobacillus* Strains. Cryst Growth Des 2(4):293–298

Cao LT, Kodera H, Abe K, Imachi H, Aoi Y, Kindaichi T, Ozaki T, Ohashi A (2015) Biological oxidation of Mn(II) coupled with nitrification for removal and recovery of minor metals by downflow hanging sponge reactor. Water Res 68:545–553

Chang Y, Bai Y, Huo Y, Qu J (2018) Benzophenone-4 promotes the growth of a Pseudomonas sp. and biogenic oxidation of Mn(II). Environ Sci Technol 52(3):1262–1269

Chidambaram D, Hennebel T, Taghavi S, Mast J, Boon N, Verstraete W, Derlelie DV, Fitts JP (2010) Concomitant microbial generation of palladium nanoparticles and hydrogen to immobilize chromate. Environ Sci Technol 44(19):7635–7640

Chowdhury M, Shoko S, Cummings F, Fester V, Ojumu TV (2017) Charge transfer between biogenic jarosite derived Fe^{3+} and TiO_2 enhances visible light photocatalytic activity of TiO_2. J Environ Sci (china) 54:256–267

Coker VS, Garrity A, Wennekes WB, Roesink HD, Cutting RS, Lloyd JR (2014) Cr(VI) and azo dye removal using a hollow-fibre membrane system functionalized with a biogenic Pd-magnetite catalyst. Environ Technol 35(5–8):1046–1054

Cutting RS, Coker VS, Fellowes JW, Lloyd JR, Vaughan DJ (2009) Mineralogical and morphological constraints on the reduction of Fe(III) minerals by *Geobacter sulfurreducens*. Geochim Cosmochim Ac 73(14):4004–4022

Cutting RS, Coker VS, Telling ND, Kimber RL, Pearce CI, Ellis BL, Lawson RS, Derlaan GV, Pattrick RAD, Vaughan DJ, Arenholz E, Lloyd JR (2010) Optimizing Cr(VI) and Tc(VII) remediation through nanoscale biomineral engineering. Environ Sci Technol 44:2577–2584

Das SK, Das AR, Guha AK (2010) Microbial synthesis of multishaped gold nanostructures. Small 6(9):1012–1021

De Corte S, Hennebel T, Fitts JP, Sabbe T, Bliznuk V, Verschuere S, van der Lelie D, Verstraete W, Boon N (2011a) Biosupported bimetallic Pd-Au nanocatalysts for dechlorination of environmental contaminants. Environ Sci Technol 45(19):8506–8513

De Corte S, Hennebel T, Verschuere S, Cuvelier C, Verstraete W, Boon N (2011b) Gold nanoparticle formation using *Shewanella oneidensis*: a fast biosorption and slow reduction process. J Chem Technol Biot 86(4):547–553

De Corte S, Sabbe T, Hennebel T, Vanhaecke L, De Gusseme B, Verstraete W, Boon N (2012) Doping of biogenic Pd catalysts with Au enables dechlorination of diclofenac at environmental conditions. Water Res 46(8):2718–2726

De Gusseme B, Hennebel T, Vanhaecke L, Soetaert M, Desloover J, Wille K, Verbeken K, Verstraete W, Boon N (2011) Biogenic palladium enhances diatrizoate removal from hospital wastewater in a microbial electrolysis cell. Environ Sci Technol 45(13):5737–5745

Du L, Xu Q, Huang M, Xian L, Feng JX (2015) Synthesis of small silver nanoparticles under light radiation by fungus *Penicillium oxalicum* and its application for the catalytic reduction of methylene blue. Mater Chem Phys 160:40–47

Du LW, Xian LA, Feng JX (2011) Rapid extra-/intracellular biosynthesis of gold nanoparticles by the fungus *Penicillium* sp. J Nanopart Res 13(3):921–930

Du ZL, Li KJ, Zhou SX, Liu XY, Yu Y, Zhang YH, He YD, Zhang YJ (2020) Degradation of ofloxacin with heterogeneous photo-Fenton catalyzed by biogenic Fe-Mn oxides. Chem Eng J 380:122427

Forrez I, Carballa M, Fink G, Wick A, Hennebel T, Vanhaecke L, Ternes T, Boon N, Verstraete W (2011) Biogenic metals for the oxidative and reductive removal of pharmaceuticals, biocides and iodinated contrast media in a polishing membrane bioreactor. Water Res 45(4):1763–1773

Forrez I, Carballa M, Noppe H, De Brabander H, Boon N, Verstraete W (2009) Influence of manganese and ammonium oxidation on the removal of 17 alpha-ethinylestradiol (EE2). Water Res 43(1):77–86

Forrez I, Carballa M, Verbeken K, Vanhaecke L, Schlusener M, Ternes T, Boon N, Verstraete W (2010) Diclofenac oxidation by biogenic manganese oxides. Environ Sci Technol 44:3449–3454

Fredrickson JK, Zachara JM, Kennedy DW, Kukkadapu RK, Mckinley JP, Heald SM, Liu CX, Plymale AE (2004) Reduction of TcO_4^- by sediment-associated biogenic Fe(II). Geochim Cosmochim Ac 68(15):3171–3187

Furgal KM, Meyer RL, Bester K (2015) Removing selected steroid hormones, biocides and pharmaceuticals from water by means of biogenic manganese oxide nanoparticles in situ at ppb levels. Chemosphere 136:321–326

Gangula A, Podila R, Ramakrishna M, Karanam L, Janardhana C, Rao AM (2011) Catalytic reduction of 4-Nitrophenol using biogenic gold and silver nanoparticles derived from *Breynia rhamnoides*. Langmuir 27(24):15268–15274

Gautam PK, Singh A, Misra K, Sahoo AK, Samanta SK (2019) Synthesis and applications of biogenic nanomaterials in drinking and wastewater treatment. J Environ Manage 231:734–748

Gericke M, Pinches A (2006) Biological synthesis of metal nanoparticles. Hydrometallurgy 83(1–4):132–140

Hargreaves JSJ, Alharthi AI (2016) Biogenic and bio-structured inorganic materials in heterogeneous catalysis: a brief overview. J Chem Technol Biot 91(2):296–303

Hennebel T, De Corte S, Vanhaecke L, Vanherck K, Forrez I, De Gusseme B, Verhagen P, Verbeken K, Van der Bruggen B, Vankelecom I, Boon N, Verstraete W (2010) Removal of diatrizoate with catalytically active membranes incorporating microbially produced palladium nanoparticles. Water Res 44(5):1498–1506

Hennebel T, De Gusseme B, Boon N, Verstraete W (2009a) Biogenic metals in advanced water treatment. Trends Biotechnol 27(2):90–98

Hennebel T, Simoen H, De Windt W, Verloo M, Boon N, Verstraete W (2009b) Biocatalytic dechlorination of trichloroethylene with bio-palladium in a pilot-scale membrane reactor. Biotechnol Bioeng 102(4):995–1002

Hennebel T, Van Nevel S, Verschuere S, De Corte S, De Gusseme B, Cuvelier C, Fitts JP, Van Der Lelie D, Boon N, Verstraete W (2011) Palladium nanoparticles produced by fermentatively cultivated bacteria as catalyst for diatrizoate removal with biogenic hydrogen. Appl Microbiol Biotechnol 91(5):1435–1445

Hennebel T, Verhagen P, Simoen H, De Gusseme B, Vlaeminck SE, Boon N, Verstraete W (2009c) Remediation of trichloroethylene by bio-precipitated and encapsulated palladium nanoparticles in a fixed bed reactor. Chemosphere 76(9):1221–1225

Hosseinkhani B, Hennebel T, Van Nevel S, Verschuere S, Yakimov MM, Cappello S, Blaghen M, Boon N (2014) Biogenic nanopalladium based remediation of chlorinated hydrocarbons in marine environments. Environ Sci Technol 48(1):550–557

Huang LB, Bai JH, Xiao R, Gao HF, Liu PP (2012) Spatial distribution of Fe, Cu, Mn in the surface water system and their effects on wetland vegetation in the Pearl River Estuary of China. Clean-Soil Air Water 40(10):1085–1092

Huo YC, Li WW, Chen CB, Li CX, Zeng R, Lau TC, Huang TY (2016) Biogenic FeS accelerates reductive dechlorination of carbon tetrachloride by *Shewanella putrefaciens* CN32. Enzyme Microb Technol 95:236–241

Iwahori K, Watanabe J, Tani Y, Seyama H, Miyata N (2014) Removal of heavy metal cations by biogenic magnetite nanoparticles produced in Fe(III)-reducing microbial enrichment cultures. J Biosci Bioeng 117(3):333–335

Jena J, Pradhan N, Nayak RR, Dash BP, Sukla LB, Panda PK, Mishra BK (2014) Microalga Scenedesmus sp.: a potential low-cost green machine for silver nanoparticle synthesis. J Microbiol Biotechn 24(4):522–533

Jung H, Kim JW, Choi H, Lee JH, Hur HG (2008) Synthesis of nano-sized biogenic magnetite and comparison of its catalytic activity in ozonation. Appl Catal B-Environ 83(3–4):208–213

Kathiraven T, Sundaramanickam A, Shanmugam N, Balasubramanian T (2015) Green synthesis of silver nanoparticles using marine algae *Caulerpa racemosa* and their antibacterial activity against some human pathogens. Appl Nanosci 5(4):499–504

Khan ME, Khan MM, Cho MH (2018) Environmentally sustainable biogenic fabrication of AuNP decorated-graphitic g-C_3N_4 nanostructures towards improved photoelectrochemical performances. RSC Adv 8(25):13898–13909

Khosro I, Nadiya J, Fataneh P, Golnaz R, Jamileh F (2013) Heavy metals resistance by bacterial strains. Ann Biol Res 4:60–63

Kim HS, Pasten PA, Gaillard JF, Stair PC (2003) Nanocrystalline todorokite-like manganese oxide produced by bacterial catalysis. J Am Chem Soc 125(47):14284–14285

Kondo K, Okamoto A, Hashimoto K, Nakamura R (2015) Sulfur-mediated electron shuttling sustains microbial long-distance extracellular electron transfer with the aid of metallic iron sulfides. Langmuir 31(26):7427–7434

Krishnaraj C, Muthukumaran P, Ramachandran R, Balakumaran MD, Kalaichelvan PT (2014) *Acalypha indica Linn*: biogenic synthesis of silver and gold nanoparticles and their cytotoxic effects against MDA-MB-231, human breast cancer cells. Biotechnol Rep 4:42–49

Kumar DA, Palanichamy V, Roopan SM (2014) Green synthesis of silver nanoparticles using *Alternanthera dentata* leaf extract at room temperature and their antimicrobial activity. Spectrochim Acta A 127:168–171

Lingamdinne LP, Chang YY, Yang JK, Singh J, Cho EH, Shiratani M, Koduru JR, Attri P (2017) Biogenic reductive preparation of magnetic inverse spinel iron oxide nanoparticles for the adsorption removal of heavy metals. Chem Eng J 307:74–84

Liu QR, Duan XG, Sun HQ, Wang YX, Tade MO, Wang SB (2016) Size-tailored porous spheres of manganese oxides for catalytic oxidation via peroxymonosulfate activation. J Phys Chem C 120(30):16871–16878

Liu W, Wang L, Wang J, Du J, Jing C (2018) New insights into microbial-mediated synthesis of Au@biolayer nanoparticles. Environ Sci-Nano 5(7):1757–1763

Lu Y, Xu L, Shu W, Zhou J, Chen X, Xu Y, Qian G (2017) Microbial mediated iron redox cycling in Fe (hydr)oxides for nitrite removal. Bioresour Technol 224:34–40

Mahdavi M, Namvar F, Ahmad MB, Mohamad R (2013) Green biosynthesis and characterization of magnetic iron oxide (Fe_3O_4) nanoparticles using seaweed (*Sargassum muticum*) aqueous extract. Molecules 18(5):5954–5964

Martins M, Mourato C, Sanches S, Noronha JP, Crespo MTB, Pereira IAC (2017) Biogenic platinum and palladium nanoparticles as new catalysts for the removal of pharmaceutical compounds. Water Res 108:160–168

Matsushita S, Komizo D, Cao LTT, Aoi Y, Kindaichi T, Ozaki N, Imachi H, Ohashi A (2018) Production of biogenic manganese oxides coupled with methane oxidation in a bioreactor for removing metals from wastewater. Water Res 130:224–233

Mertens B, Blothe C, Windey K, De Windt W, Verstraete W (2007) Biocatalytic dechlorination of lindane by nano-scale particles of Pd(0) deposited on *Shewanella oneidensis*. Chemosphere 66(1):99–105

Murphy CJ, San TK, Gole AM, Orendorff CJ, Gao JX, Gou L, Hunyadi SE, Li T (2005) Anisotropic metal nanoparticles: synthesis, assembly, and optical applications. J Phys Chem B 109(29):13857–13870

Muthukumar H, Gire A, Kumari M, Manickam M (2017) Biogenic synthesis of nano-biomaterial for toxic naphthalene photocatalytic degradation optimization and kinetics studies. Int Biodeter Biodegr 119:587–594

Nelson YM, Lion LW, Shuler ML, Ghiorse WC (2002) Effect of oxide formation mechanisms on lead adsorption by biogenic manganese (Hydr)oxides, iron (Hydr)oxides, and their mixtures. Environ Sci Technol 36:421–425

Nishi R, Kitjanukit S, Nonaka K, Okibe N (2020) Oxidation of arsenite by self-regenerative bioactive birnessite in a continuous flow column reactor. Hydrometallurgy 196:105416

Nitzsche KS, Weigold P, Losekann-Behrens T, Kappler A, Behrens S (2015) Microbial community composition of a household sand filter used for arsenic, iron, and manganese removal from groundwater in Vietnam. Chemosphere 138:47–59

Noman M, Shahid M, Ahmed T, Niazi MBK, Hussain S, Song F, Manzoor I (2020) Use of biogenic copper nanoparticles synthesized from a native Escherichia sp as photocatalysts for azo dye degradation and treatment of textile effluents. Environ Pollut 257:113514

Nutt MO, Hughes JB, Wong MS (2005) Designing Pd-on-Au bimetallic nanoparticle catalysts for trichloroethene hydrodechlorination. Environ Sci Technol 39(5):1346–1353

Parshetti GK, Doong RA (2008) Immobilization of bimetallic nanoparticles on microfiltration membranes for trichloroethylene dechlorination. Water Sci Technol 58(8):1629–1636

Pham VL, Kim DG, Ko SO (2020) Advanced oxidative degradation of acetaminophen by carbon catalysts: radical vs non-radical pathways. Environ Res 188:109767

Pi K, Wang Y, Xie X, Ma T, Liu Y, Su C, Zhu Y, Wang Z (2017) Remediation of arsenic-contaminated groundwater by in-situ stimulating biogenic precipitation of iron sulfides. Water Res 109:337–346

Parandhaman T, Dey MD, Das SK (2019) Biofabrication of supported metal nanoparticles: exploring the bioinspiration strategy to mitigate the environmental challenges. Green Chem 21:5469–5500

Prasad TNVKV, Kambala VSR, Naidu R (2012) Phyconanotechnology: synthesis of silver nanoparticles using brown marine algae *Cystophora moniliformis* and their characterisation. J Appl Phycol 25(1):177–182

Qu X, Alvarez PJ, Li Q (2013) Applications of nanotechnology in water and wastewater treatment. Water Res 47(12):3931–3946

Qu YY, Shen WL, Pei XF, Ma F, You SN, Li SZ, Wang JW, Zhou JT (2017) Biosynthesis of gold nanoparticles by *Trichoderma* sp WL-Go for azo dyes decolorization. J Environ Sci 56:79–86

Rajeshkumar S, Bharath LV (2017) Mechanism of plant-mediated synthesis of silver nanoparticles - a review on biomolecules involved, characterisation and antibacterial activity. Chem-Biol Interact 273:219–227

Rentz JA, Turner IP, Ullman JL (2009) Removal of phosphorus from solution using biogenic iron oxides. Water Res 43(7):2029–2035

Roberts J, Kumar A, Du J, Hepplewhite C, Ellis DJ, Christy AG, Beavis SG (2016) Pharmaceuticals and personal care products (PPCPs) in Australia's largest inland sewage treatment plant, and its contribution to a major Australian river during high and low flow. Sci Total Environ 541:1625–1637

Roberts LC, Hug SJ, Ruettimann T, Billah MM, Khan AW, Rahman MT (2004) Arsenic removal with iron(II) and iron(III) in waters with high silicate and phosphate concentrations. Environ Sci Technol 38:307–315

Sadhasivam S, Vinayagam V, Balasubramaniyan M (2020) Recent advancement in biogenic synthesis of iron nanoparticles. J Mol Struct 1217:128372

Saputra E, Muhammad S, Sun HQ, Ang HM, Tade MO, Wang SB (2013) Manganese oxides at different oxidation states for heterogeneous activation of peroxymonosulfate for phenol degradation in aqueous solutions. Appl Catal B-Environ 142:729–735

Saputra E, Muhammad S, Sun HQ, Ang HM, Tade MO, Wang SB (2014) Shape-controlled activation of peroxymonosulfate by single crystal alpha-Mn_2O_3 for catalytic phenol degradation in aqueous solution. Appl Catal B-Environ 154:246–251

Sarkar J, Ray S, Chattopadhyay D, Laskar A, Acharya K (2012) Mycogenesis of gold nanoparticles using a phytopathogen *Alternaria alternata*. Bioproc Biosyst Eng 35(4):637–643

Shahverdi AR, Minaeian S, Shahverdi HR, Jamalifar H, Nohi AA (2007) Rapid synthesis of silver nanoparticles using culture supernatants of *Enterobacteria*: a novel biological approach. Process Biochem 42(5):919–923

Shankar PD, Shobana S, Karuppusamy I, Pugazhendhi A, Ramkumar VS, Arvindnarayan S, Kumar G (2016) A review on the biosynthesis of metallic nanoparticles (gold and silver) using bio-components of microalgae: formation mechanism and applications. Enzyme Microb Technol 95:28–44

Sinha SN, Paul D, Halder N, Sengupta D, Patra SK (2014) Green synthesis of silver nanoparticles using fresh water green alga Pithophora oedogonia (Mont) Wittrock and evaluation of their antibacterial activity. Appl Nanosci 5(6):703–709

Sintubin L, De Gusseme B, Van der Meeren P, Pycke BF, Verstraete W, Boon N (2011) The antibacterial activity of biogenic silver and its mode of action. Appl Microbiol Biotechnol 91(1):153–162

Soumya M, Rajeshkumar S, Kumar SV (2017) A review on biogenic synthesis of gold nanoparticles, characterization, and its applications. Resour Effic Technol 3(4):516–527

Sowani H, Mohite P, Damale S, Kulkarni M, Zinjarde S (2016) Carotenoid stabilized gold and silver nanoparticles derived from the *Actinomycete Gordonia amicalis* HS-11 as effective free radical scavengers. Enzyme Microb Technol 95:164–173

Spiro TG, Bargar JR, Sposito G, Tebo BM (2010) Bacteriogenic Manganese Oxides Accounts Chem Res 43:2–9

Srinath BS, Ravishankar Rai V (2015) Rapid biosynthesis of gold nanoparticles by *Staphylococcus epidermidis*: its characterisation and catalytic activity. Mater Lett 146:23–25

Srivastava SK, Yamada R, Ogino C, Kondo A (2013) biogenic synthesis and characterization of gold nanoparticles by *Escherichia coli* K12 and its heterogeneous catalysis in degradation of 4-nitrophenol. Nanoscale Res Lett 8(70):1–9

Suja E, Nancharaiah YV, Venugopalan VP (2014) Biogenic nanopalladium production by self-immobilized granular biomass: application for contaminant remediation. Water Res 65:395–401

Suresh AK, Pelletier DA, Wang W, Broich ML, Moon JW, Gu BH, Allison DP, Joy DC, Phelps TJ, Doktycz MJ (2011) Biofabrication of discrete spherical gold nanoparticles using the metal-reducing bacterium *Shewanella oneidensis*. Acta Biomater 7(5):2148–2152

Suvith VS, Philip D (2014) Catalytic degradation of methylene blue using biosynthesized gold and silver nanoparticles. Spectrochim Acta A 118:526–532

Takahashi Y, Manceau A, Geoffroy N, Marcus MA, Usui A (2007) Chemical and structural control of the partitioning of Co, Ce, and Pb in marine ferromanganese oxides. Geochim Cosmochim Ac 71(4):984–1008

Tanaka K, Tani Y, Takahashi Y, Tanimizu M, Suzuki Y, Kozai N, Ohnuki T (2010) A specific Ce oxidation process during sorption of rare earth elements on biogenic Mn oxide produced by Acremonium sp. strain KR21–2. Geochim Cosmochim Ac 74(19):5463–5477

Tani Y, Ohashi M, Miyata N, Seyama H, Iwahori K, Soma M (2004) Sorption of Co(II), Ni(II), and Zn(II) on biogenic manganese oxides produced by a Mn-oxidizing fungus, strain KR21-2. J Environ Sci Health Part A 39(10):2641–1660

Tebo BM, Johnson HA, McCarthy JK, Templeton AS (2005) Geomicrobiology of manganese(II) oxidation. Trends Microbiol 13(9):421–428

Tian N, Tian X, Nie Y, Yang C, Zhou Z, Li Y (2018) Biogenic manganese oxide: an efficient peroxymonosulfate activation catalyst for tetracycline and phenol degradation in water. Chem Eng J 352:469–476

Tran TN, Kim DG, Ko SO (2018) Synergistic effects of biogenic manganese oxide and Mn(II)-oxidizing bacterium *Pseudomonas putida* strain MnB1 on the degradation of 17 α-ethinylestradiol. J Hazard Mater 344:350–359

Tuo Y, Liu G, Dong B, Zhou J, Wang A, Wang J, Jin R, Lv H, Dou Z, Huang W (2015) Microbial synthesis of Pd/Fe_3O_4, Au/Fe_3O_4 and PdAu/Fe_3O_4 nanocomposites for catalytic reduction of nitroaromatic compounds. Sci Rep 5:13515

Vázquez-Morillas A, Vaca-Mier M, Alvarez PJ (2006) Biological activation of hydrous ferric oxide for reduction of hexavalent chromium in the presence of different anions. Eur J Soil Biol 42(2):99–106

Veeramani H, Alessi DS, Suvorova EI, Lezama-Pacheco JS, Stubbs JE, Sharp JO, Dippon U, Kappler A, Bargar JR, Bernier-Latmani R (2011) Products of abiotic U(VI) reduction by biogenic magnetite and vivianite. Geochim Cosmochim Ac 75(9):2512–2528

Veeramani H, Scheinost AC, Monsegue N, Qafoku NP, Kukkadapu R, Newville M, Lanzirotti A, Pruden A, Murayama M, Hochella MF (2013) Abiotic reductive immobilization of U(VI) by biogenic mackinawite. Environ Sci Technol 47(5):2361–2369

Venkatesan J, Manivasagan P, Kim SK, Kirthi AV, Marimuthu S, Rahuman AA (2014) Marine algae-mediated synthesis of gold nanoparticles using a novel *Ecklonia cava*. Bioproc Biosyst Eng 37(8):1591–1597

Villalobos M, Bargar J, Sposito G (2005) Mechanisms of Pb(II) sorption on a biogenic manganese oxide. Environ Sci Technol 39(2):569–576

Wang D, Ao Y, Wang P (2020) Effective inactivation of Microcystis aeruginosa by a novel Z-scheme composite photocatalyst under visible light irradiation. Sci Total Environ 746:141149

Wang R, Wang S, Tai Y, Tao R, Dai Y, Guo J, Yang Y, Duan S (2017) Biogenic manganese oxides generated by green algae *Desmodesmus* sp. WR1 to improve bisphenol A removal. J Hazard Mater 339:310–319

Wang W, Shao Z, Liu Y, Wang G (2009) Removal of multi-heavy metals using biogenic manganese oxides generated by a deep-sea sedimentary bacterium - *Brachybacterium* sp. strain Mn32. Microbiology 155:1989–1996

Wang YX, Sun HQ, Ang HM, Tade MO, Wang SB (2015) 3D-hierarchically structured MnO_2 for catalytic oxidation of phenol solutions by activation of peroxymonosulfate: Structure dependence and mechanism. Appl Catal B-Environ 164:159–167

Watanabe J, Tani Y, Chang JN, Miyata N, Naitou H, Seyama H (2013) As(III) oxidation kinetics of biogenic manganese oxides formed by *Acremonium strictum* strain KR21-2. Chem Geol 347:227–232

Watts MP, Coker VS, Parry SA, Pattrick RAD, Thomas RAP, Kalin R, Lloyd JR (2015) Biogenic nano-magnetite and nano-zero valent iron treatment of alkaline Cr(VI) leachate and chromite ore processing residue. Appl Geochem 54:27–42

Whitaker AH, Peña J, Amor M, Duckworth OW (2018) Cr(VI) uptake and reduction by biogenic iron (oxyhydr)oxides. Environ Sci-Proc Imp 20(7):1056–1068

Windt WD, Aelterman P, Verstraete W (2005) Bioreductive deposition of palladium (0) nanoparticles on Shewanella oneidensis with catalytic activity towards reductive dechlorination of polychlorinated biphenyls. Environ Microbiol 7(3):314–325

Wright MH, Farooqui SM, White AR, Greene AC (2016) Production of manganese oxide nanoparticles by *Shewanella* species. Appl Environ Microbiol 82(17):5402–5409

Xie J, Lee JY, Wang DIC, Ting YP (2007) Identification of active biomolecules in the high-yield synthesis of single-crystalline gold nanoplates in algal solutions. Small 3(4):672–682

Xie Y, Li P, Zeng Y, Li X, Xiao Y, Wang Y, Zhang Y (2018) Thermally treated fungal manganese oxides for bisphenol A degradation using sulfate radicals. Chem Eng J 335:728–736

Zhang X, Qu Y, Shen W, Wang J, Li H, Zhang Z, Li S, Zhou J (2016) Biogenic synthesis of gold nanoparticles by yeast *Magnusiomyces ingens* LH-F1 for catalytic reduction of nitrophenols. Colloid Surface A 497:280–285

Zhang Y, Zhu H, Szewzyk U, Geissen SU (2015a) Removal of pharmaceuticals in aerated biofilters with manganese feeding. Water Res 72:218–226

Zhang Y, Zhu H, Szewzyk U, Lübbecke S, Uwe Geissen S (2017) Removal of emerging organic contaminants with a pilot-scale biofilter packed with natural manganese oxides. Chem Eng J 317:454–460

Zhang Z, Zhang ZM, Chen H, Liu J, Liu C, Ni H, Zhao CS, Ali M, Liu F, Li L (2015b) Surface Mn(II) oxidation actuated by a multicopper oxidase in a soil bacterium leads to the formation of manganese oxide minerals. Sci Rep 5:1–13

Zhang ZL, Hong HS, Zhou JL, Huang J, Yu G (2003) Fate and assessment of persistent organic pollutants in water and sediment from Minjiang River Estuary. Southeast China Chemosphere 52(9):1423–1430

Zheng H, Tani Y, Naitou H, Miyata N, Tojo F (2016) Oxidative Ce^{3+} sequestration by fungal manganese oxides with an associated Mn(II) oxidase activity. Appl Geochem 71:110–122

Zhou H, Pan H, Xu J, Xu W, Liu L (2016) Acclimation of a marine microbial consortium for efficient Mn(II) oxidation and manganese containing particle production. J Hazard Mater 304:434–440

Zhou NQ, Liu DF, Min D, Cheng L, Huang XN, Tian LJ, Li DB, Yu HQ (2018) Continuous degradation of ciprofloxacin in a manganese redox cycling system driven by *Pseudomonas putida* MnB-1. Chemosphere 211:345–351